Applied Energy, Volume 249, 1 September 2019, Pages 237-244
DOI:10.1016/j.apenergy.2019.04.096

Gas-fired chemical looping combustion with supercritical CO_2 cycle

Navid Khallaghi, Dawid P. Hanak, Vasilije Manovic*

Energy and Power, School of Water, Energy and Environment,
Cranfield University,
Bedford, Bedfordshire, MK43 0AL, UK

*Corresponding author: *Dawid P. Hanak, d.p.hanak@cranfield.ac.uk*

Abstract

Oxy-fuel combustion is currently gathering attention as one of the promising options for capturing CO_2 efficiently, when applied to power plants, for subsequent carbon sequestration. However, this option requires a large quantity of high-purity oxygen that is usually produced in an energy-intensive air separation unit (ASU). Chemical looping combustion (CLC) is a technology with the potential of reducing the costs and energy penalties associated with current state-of-the-art cryogenic ASUs. In this work, the techno-economic performance of a natural gas-fired oxy-combustion cycle with cryogenic ASU is compared with that based on CLC. Two natural gas-fired cycles are considered: (i) staged oxy-fuel natural gas combined cycle as a reference; and (ii) gas-fired CLC with supercritical CO_2 cycle. The process models were developed in Aspen Plus® in order to evaluate the thermodynamic performance of the proposed system and to benchmark it against the reference cycle. The results show that the net efficiency of the proposed cycle, including CO_2 compression, is more than 51%, which is comparable to that of a conventional natural gas combined cycle with CO_2 capture and 2.7% points higher than that of the reference cycle. Moreover, the economic evaluation indicates that a reduction in levelised cost of electricity from £38.3/MWh to £36.1/MWh can be achieved by replacement of the ASU-based oxy-fuel system with CLC. Hence, gas-fired CLC with a supercritical CO_2 cycle has high potential for commercialisation.

Key words: Carbon capture, oxy-fuel turbine, cryogenic ASU, chemical looping combustion, natural gas combined cycle, oxygen production

1. Introduction

Carbon capture and storage (CCS) is increasingly regarded as an effective option to limit greenhouse gas emissions, while still maintaining the ability of utilising fossil fuels for power generation. The potential strategies proposed for CCS include pre-combustion, post-combustion and oxy-combustion [1].

Oxy-combustion has become one of the most promising options applicable to power generation systems [2]. This technology involves the process of fuel combustion in a high-purity O_2 environment that results in the flue gas containing mostly pure CO_2 after water vapour has been separated by condensation. Importantly, fuel combustion under such conditions would result in intolerably high temperatures in the combustors, reaching more than 2000°C. Therefore, some fraction of the exhaust gas is recycled back into the combustor to moderate the flame temperature.

It needs to be stressed, however, that the oxy-combustion process requires high O_2 production capacity, as for a 500 MW_e power plant the O_2 requirement is almost 10,000 t/d [3]. Currently, the cryogenic air separation unit (ASU) is the only commercially applied and mature technology that is capable of producing such large quantities of O_2 at high purity [4], but it is a complex and energy-intensive technology, the power requirement for which is about 200 kWh/tO_2 at 95%$_{vol}$ O_2 purity [5].

In chemical looping combustion (CLC), O_2 is separated from the air and then transported to the fuel via an oxygen carrier (OC). In its preferred embodiment, CLC consists of two interconnected fluidised bed reactors: an air reactor and a fuel reactor. O_2 separated from the air in the air reactor is transferred by OCs to the fuel reactor [6]. The chemical reactions in the air and fuel reactors, respectively, are as follows:

$$Me_xO_{y-2}(s) + Air(g) \longrightarrow Me_xO_y(s) + Oxygen\ depleted\ air\ (g) \quad \text{(R1)}$$

$$Me_xO_y(s) + fuel \longrightarrow Me_xO_{y-2}(s) + Combustion\ products\ (g) \quad \text{(R2)}$$

The reduced OC is then recycled to the air reactor. The gas stream leaving the fuel reactor comprises mainly CO_2 and water vapour. The benefit of using CLC is that the combustion products (CO_2 and water vapour) are inherently separated from other components such as N_2 and Ar. Hence, unlike in the case of post-combustion capture (PCC), no additional energy is required for CO_2 separation [7].

CLC is a promising technology [8] which has been developed for combustion of gaseous, liquid and solid fuels and is undergoing significant scale-up at present [9]. The largest (120 kW) gas-based CLC system is located at the Vienna University of Technology [10]. Furthermore, a number of OCs have been thoroughly studied. Källén et al. [11,12] tested calcium manganite in a 10 kW pilot-scale CLC unit and iron/manganese/silicon-based OCs in a 300 W lab-scale CLC unit. All performed well with respect to gas conversion, achieving high O_2 transport capacity. Furthermore, regarding the performance of different CLC configurations, Brandvoll and Bolland [13] revealed that a net efficiency of 54% was obtainable with integration of CLC to a humid air turbine cycle. Naqvi and Bolland [14] showed that using CLC in the conventional combined cycle can result in a net efficiency of 53%, including CO_2 compression. Chen et al. [15] analysed the possibilities and benefits of integration of CLC with supercritical CO_2 for combined heat and power cogeneration. Their proposed cycle reached a net power efficiency of 41.3% with a heating efficiency of 40.4%. However, the economic feasibility of such concept has not yet been proven. Spallina et al. [16] performed a thermodynamic analysis on the integration of solid oxide fuel cells (SOFCs) with CLC in natural gas-fired power plants. The integrated plant showed a net efficiency in the range of 63-70%. Hamers et al. [17] analysed a two-stage CLC integrated with a coal gasification plant. They revealed that a two-stage CLC can achieve a net efficiency of about 40% and results in significantly lower reactor cost compared to a single-stage CLC. Olaleye and Wang [18] performed an economic analysis of a CLC unit integrated with a humid air turbine that was characterised with an efficiency of 57.1%. Their study has shown that for a 50 MW_{th} plant, the capital cost and net present value are £52M and £104M, respectively, assuming a cost of electricity of £77.5/MWh. However, to support commercialisation of the CLC technology, its techno-economic feasibility needs to be further evaluated, especially considering advanced power cycles, such as the supercritical CO_2 cycle (sCO_2) that is considered as a suitable replacement for conventional steam cycles [19].

This work evaluates the techno-economic feasibility of integrating CLC with the sCO_2 cycle to achieve high efficiency with low CO_2 emissions and affordable electricity cost. A novel gas-fired chemical looping combustion process with supercritical CO_2 cycle (CLC-sCO_2) is proposed and its performance is benchmarked against staged oxy-fuel natural gas combined cycle (SOF-NGCC). The process model of the CLC-sCO_2 is

developed in Aspen Plus®. Parametric studies are performed to determine the optimum thermodynamic performance, characterised with the highest net efficiency. Finally, the economic feasibility of the considered cycles is evaluated and compared in terms of capital cost and levelised cost of electricity. Therefore, this work demonstrates the advantage of using CLC instead of an ASU-based oxy-fuel combustor for high-efficiency low-CO_2-emission power generation. It also proves the economic feasibility of linking CLC with the sCO_2 cycle that is characterised by a higher efficiency and smaller size compared to other cycles, such as the conventional steam cycle. Such information on process design, operation, and techno-economic feasibility will support further development of CLC for power generation.

2. Process description and simulation

Figure 1 presents a schematic of the SOF-NGCC. The entire quantity of high-purity O_2, required to ensure complete combustion, enters into the first combustion stage, whereas natural gas enters into each of three combustion stages with nearly equal feed rates. The combustion products of the first stage, along with unreacted O_2, act as a diluent for the second-stage combustion. Additionally, to maintain the desired combustion temperature of the topping cycle, excess heat is extracted from the first stage to pre-heat the CO_2 stream in the sCO_2 cycle primarily by radiation as described by Gopan et al. [20,21]. Absence of the exhaust gas recycle (EGR) results in a high combustion temperature and heat transfer. This may result in a high surface temperature that may exceed allowable operating limits. This challenge is addressed by staging the delivery of the fuel and controlling the characteristics of the flame [22]. This process continues until O_2 is almost entirely (except for 5% excess O_2) consumed at the last combustion stage. The exhaust gas, which is mainly composed of water vapour and CO_2, is expanded in the turbine to generate power. The flue gas then passes through a heat exchanger and transfers heat to the O_2, fuel and CO_2 streams in the sCO_2 cycle. The water vapour is easily separated from the cold flue gas and the remaining CO_2 is sent to the carbon purification unit (CPU) to be conditioned for storage. In the bottoming cycle, the sCO_2 stream is first pressurised to 300 bar and then preheated in a high-temperature recuperator (HTR) and low-temperature recuperator (LTR), as well as multi-stage combustor, before entering the high-

pressure CO_2 turbine. A detailed description of SOF-NGCC is presented in Khallaghi et al. [23].

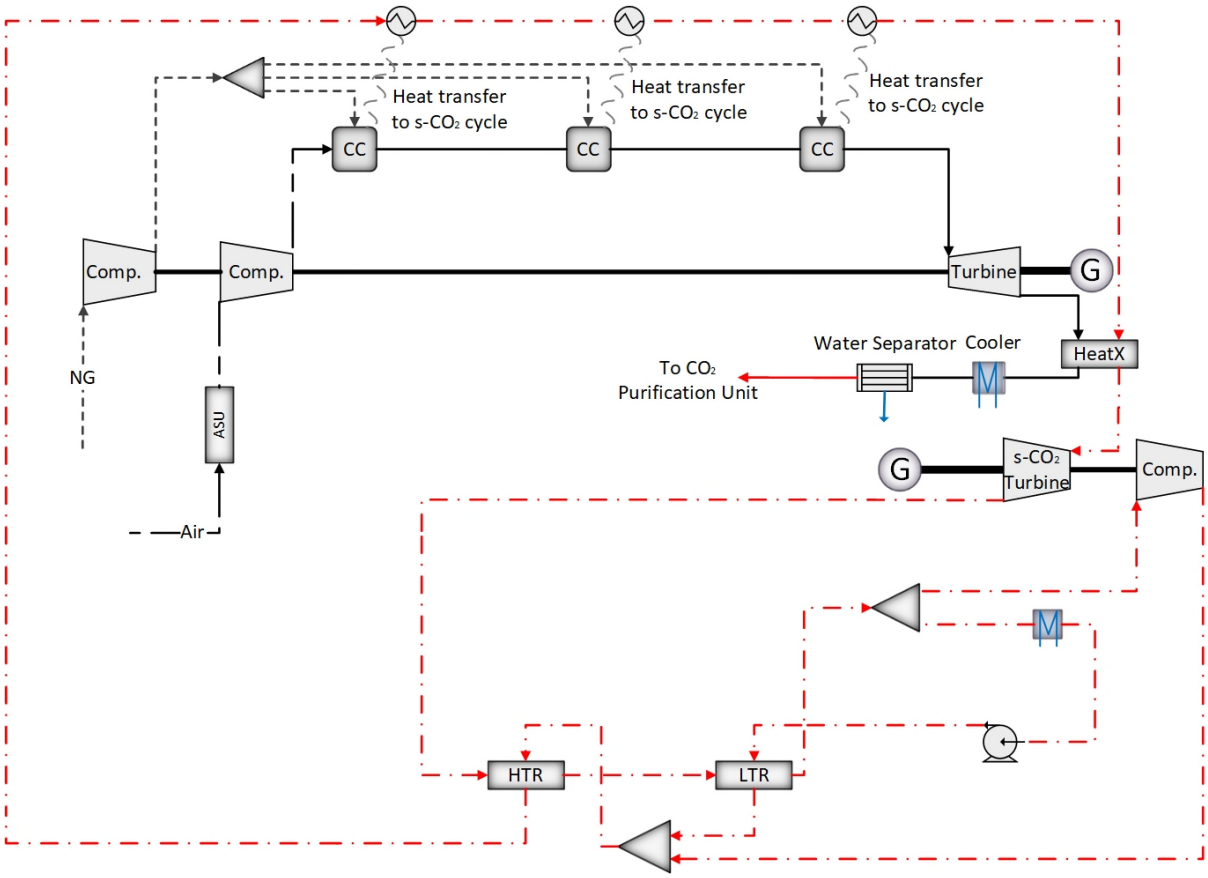

Figure 1. Schematic of SOF-NGCC.

As shown in Figure 2, the CLC-sCO_2 power section is the same as the closed sCO_2 cycle used as a bottoming cycle in the SOF-NGCC. Conversely, the heat is transferred indirectly from two fluidised bed reactors, oxygen-depleted air and exhaust gas to the sCO_2 cycle. Then, the hot sCO_2 enters the high-pressure CO_2 turbine. Two reactors work at considerably lower pressure (1.25 bar) than that in SOF-NGCC combustors (300 bar). Although this results in no power obtained from exhaust gas and oxygen-depleted air leaving the reactors, it is expected that such reactors will have a significantly smaller capital cost. Finally, to ensure that the separated CO_2 leaves the system at the pressure required for its storage, the CO_2 stream is pressurised to 120 bar after water separation.

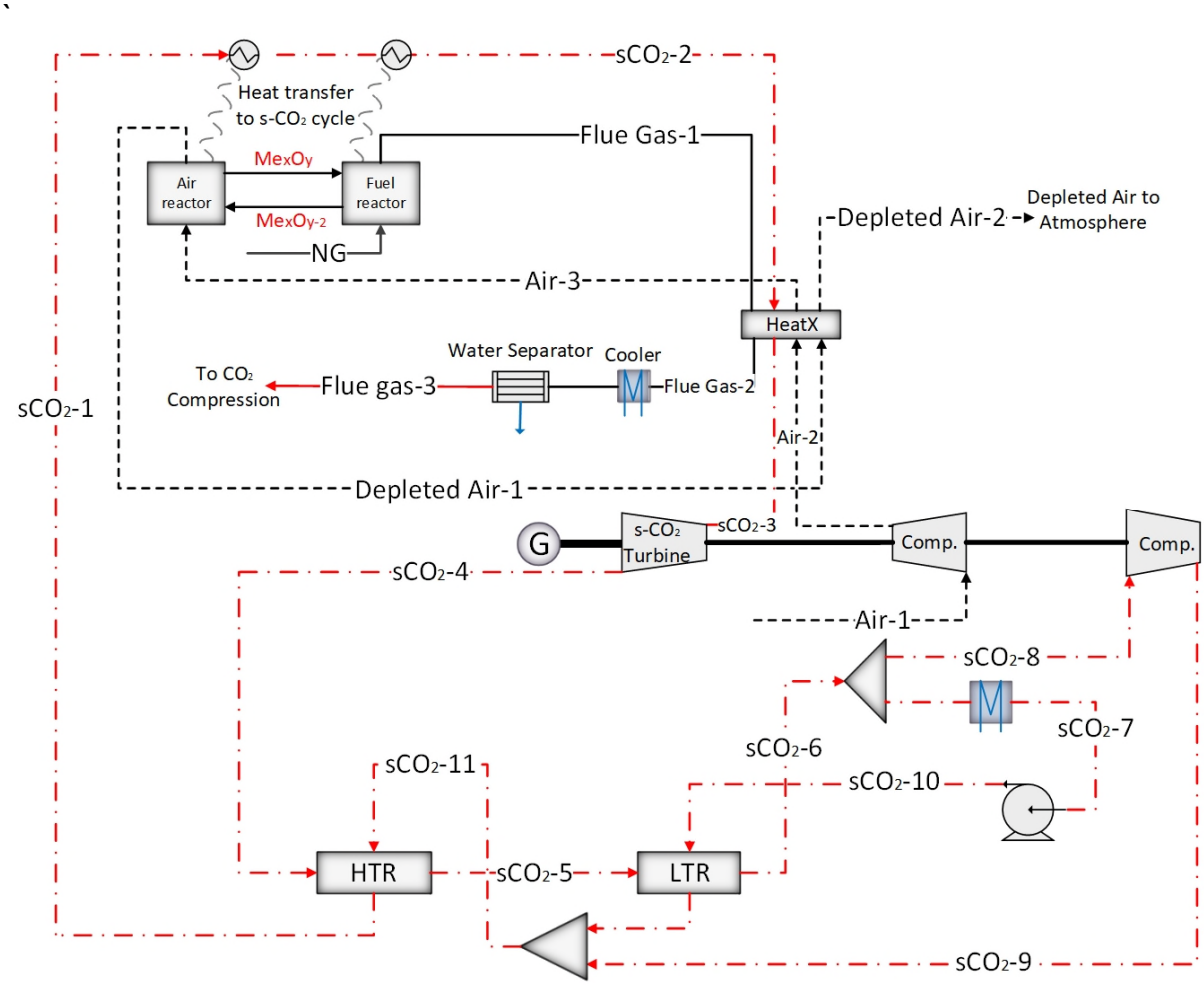

Figure 2. Schematic of CLC-sCO$_2$ (sCO$_2$ gains heat, Depleted Air-1 loses heat, Flue gas-1 loses heat, Air-2 gains heat, sCO$_2$-4 loses heat, sCO$_2$-5 loses heat)

2.1. Model development

The process model for CLC-sCO$_2$ has been developed in Aspen Plus®. The package used for the thermodynamic property estimation is the Peng Robinson equation of state which is suitable for hydrocarbons and light gases, such as CO$_2$ and H$_2$ [24]. All components are defined as conventional except for OCs which are solid. The reactors are modelled as Gibbs reactors (*RGibbs*), which assume chemical and phase equilibrium based on Gibbs energy minimisation [25]. Importantly, it is assumed that heat loss is negligible. All heat exchangers are modelled using the *MHeatX* block and designed based on the assumption that the minimum temperature approach of the heat exchangers is 5°C, similarly to previous studies on the sCO$_2$ cycle [26,27]. Similarly to the study by Hanak and Manovic [19] and Le Moullec [28], it is assumed

that high-pressure CO_2 in the sCO_2 cycle is heated in the CLC reactors. All turbines are modelled as individual turbine sections using the *Compr* block. Cu has been selected as OC for this study due to its high reaction rate, high O_2 transport capacity and its complementary combustion thermodynamics that completely convert fuel to CO_2 and water vapour [29,30]. It is assumed that the agglomeration rate of Cu is negligible. Moreover, due to the high oxidation conversion rate of Cu [31] and its high combustion temperature, it is assumed that the complete oxidation of Cu occurs [32]. The properties of the natural gas, key assumptions used in modelling, the turbomachinery and initial simulation parameters for the CLC-sCO_2 are summarised in Table 1.

Importantly, the SOF-NGCC, which has been thermodynamically analysed by Khallaghi et al. [23], is selected as a reference cycle in this study. To have a fair comparison between CLC-sCO_2 and the reference cycle, the SOF-NGCC simulation is adapted to the new assumptions mentioned in Table 1.

Table 1. Main assumptions and turbomachinery specification for simulation

Parameter	Value
Natural gas composition and conditions [23]	
Methane ($\%_{vol}$)	89
Ethane ($\%_{vol}$)	7
Propane ($\%_{vol}$)	1
Butane ($\%_{vol}$)	0.1
Pentane ($\%_{vol}$)	0.01
CO_2 ($\%_{vol}$)	2
N_2 ($\%_{vol}$)	0.89
Lower Heating Value (LHV) (MJ/kg)	46.50
Temperature (°C)	15
Pressure (bar)	1.25
Turbomachinery specification	
Isentropic efficiency of pump (%) [33]	90
Isentropic efficiency of turbine (%) [33]	93
Isentropic efficiency of compressor (%) [33]	89
Mechanical efficiency of compressors and pump (%) [34]	99.6
Electrical efficiency of generator (%) [35]	98.5
Initial CLC-sCO_2 operating parameters	
Oxygen carrier type	Cu/CuO
Oxygen carrier mass flow rate (kg/s)	350*
Combustors (oxidation and reduction) pressure (bar)	1.25
Combustors and reactor pressure drop (mbar)	150
Pressure drop in heat exchangers (%)	1
Oxidation reactor temperature (°C)	995
Reduction reactor temperature (°C)	900
Turbine backpressure (bar)	35
sCO_2 turbine inlet temperature (°C)	700
sCO_2 turbine inlet pressure (bar)	300
sCO_2 turbine backpressure (bar)	75
Recompression split fraction (-)	0.3

*Assumption is made based on fully oxidised oxygen carrier flowing into the fuel reactor.

2.2. Model validation

The considered process consists of two parts: (i) the power generation, which is based on the sCO_2 cycle, and, (ii) CLC that converts the chemical energy of natural gas into heat for the sCO_2 cycle. Importantly, the prediction of the CLC model is comparable to that presented in the work by Mantripragada and Rubin [10]. The sCO_2 cycle has been developed based on the recompression sCO_2 cycle from Moisseytsev and Sienicki [36] and has been validated by Hanak and Manovic [19]. As this study considers a pump in place of the main compressor, the data from Moisseytsev and Sienicki [36] are used as a benchmark for the prediction of the sCO_2 cycle model used in this study (Table 2).

Table 2. Benchmark of the sCO_2 cycle stream data with Moisseytsev and Sienicki [36].

Stream	Temperature		Pressure	
	Literature	Model	Literature	Model
sCO_2-7	31.3	31	74.0	75
sCO_2-10	84.4	52	200.0	200
sCO_2-11	171.8	178	199.6	198
sCO_2-1	323.3	317	199.1	196
sCO_2-3	471.8	472	198.4	198
sCO_2-4	362.3	364	77.3	77
sCO_2-5	190.7	190	76.9	76
sCO_2-6	90.2	85	76.3	75

Using the maximum cycle pressure of 200 bar for the stream entering LTR and sCO_2 turbine inlet temperature of 472°C as in Moisseytsev and Sienicki [36], the temperatures and pressures of the streams in the sCO_2 cycle are compared with the data reported in that study. The main reasons for such a deviation are different turbomachinery efficiencies and pressure drops considered in this study compared to those in Moisseytsev and Sienicki [36]. Moreover, a pump and a compressor are used in this study instead of two compressors for the compression stage. This resulted in a lower temperature of the CO_2 stream entering the LTR. Nevertheless, the model prediction was found to be in good agreement with the literature data.

3. Techno-economic performance indicators

To evaluate the thermodynamic performance of the CLC-sCO_2, the thermal efficiency of the system is defined in Eq. (1) as the ratio of the net power output ($\dot{W}_{net}$), which is calculated as the gross power output less the system's parasitic load, and the chemical energy input to the system, that is defined as the product of the fuel consumption rate ($\dot{m}_{fuel}$) and its lower heating value (LHV). The gross power output of the CLC-sCO_2 is the electric power output of the generator linked with the sCO_2 turbine through the mechanical shaft. Importantly, the parasitic load is the sum of all parasitic loads of the entire cycle associated with its compressors and pumps.

$$\eta_{net} = \frac{\dot{W}_{net}}{\dot{m}_{fuel} \cdot LHV} \quad (1)$$

The economic performance of the considered cases is evaluated using the levelised cost of electricity (LCOE), defined in Eq. (2). This equation is based on the assumption that the capital cost of the proposed process is completely covered by the revenue from electricity sales. Therefore, the LCOE indicates the minimum electricity price required for the system to become economically feasible. This approach correlates the net power output, net thermal efficiency, and capacity factor (CF) with economic performance indicators, such as total capital requirement (TCR), variable (VOM) and fixed (FOM) operating and maintenance costs, specific fuel cost (SFC) and the fixed charge factor (FCF). The main assumptions for the economic analysis are described in Table 3.

$$LCOE = \frac{TCR \times FCF + FOM}{8760 \times \dot{W}_{net} \times CF} + \frac{SFC}{\eta_{net}} + VOM \quad (2)$$

Table 3. Assumptions for the economic analysis [34]

Parameter	Value
Variable operating cost as a fraction of total capital cost (%)	2.0
Fixed operating cost as a fraction of total capital cost (%)	1.0
Natural gas price (£/GJ)	3.0
Plant lifetime (years)	25
Project interest rate (%)	8.75
Capacity factor (%)	80

Importantly, FCF, which divides the total capital cost into uniform annual amounts over the project lifetime, is calculated using Eq. (3) considering the project interest rate (r) and project lifetime (T). Finally, the annual net electricity generation, FCF along with the fuel costs, and operating and maintenance costs, are assumed to be constant for the project lifetime.

$$\boldsymbol{FCF = \frac{r(1+r)\,T}{(1+r)\,T - 1}} \quad (3)$$

The capital costs for the considered cases are estimated using the bottom-up approach, considering the individual capital costs of the key equipment. The capital costs for combustors in the SOF-NGCC and reactors in the CLC-sCO_2 are estimated

using the component scaling factor, as shown in Eq. (4). In the latter case, both reactors are assumed to be fluidised bed reactors. Having assumed that the residence times for the air reactor and fuel reactor are 5 and 60 seconds [37], respectively, the volume for each reactor is calculated using the procedure described by Lyngfelt et al. [38]**.** Then, the weight for each reactor is calculated as presented in Peters and Timmerhaus [39]. Thereafter, by considering reactors described by NRE [40] as a reference and using the scaling factor of 0.67, the capital cost of both CLC reactors is estimated. On the other hand, the reference for capital cost of combustors used in the SOF-NGCC is selected from López et al. [41]. Considering the total outlet mass flow rate as a scaling parameter and the scaling factor of 0.6, the cost for the combustor in the SOF-NGCC is calculated.

$$\begin{aligned} &\boldsymbol{cost\ of\ equipment\ A} \\ &\quad = (\boldsymbol{cost\ of\ equipment\ A_{ref}}) \\ &\quad \times \left(\frac{\boldsymbol{capacity\ of\ A}}{\boldsymbol{capacity\ of\ A_{ref}}}\right)^{\boldsymbol{scaling\ factor}} \end{aligned} \tag{4}$$

The capital cost of the SOF-NGCC topping cycle is determined based on the capital cost correlations for specific pieces of equipment, using the bottom-up approach. These correlations were taken from the literature and are gathered in Table 4.

Table 4. Capital cost estimation for SOF-NGCC topping cycle

Equipment [scaling parameter]	Correlation
Fuel compressor [Brake power requirement, $\dot{W}_{FC,BRK}$ (kW)] [42,43]	$C_C = 91,562\ (\frac{\dot{W}_{FC,BRK}}{445})^{0.67}$
Air/O_2 compressor [Brake power requirement, $\dot{W}_{AC,BRK}$ (kW)] [42,43]	$C_C = 91,562\ (\frac{\dot{W}_{AC,BRK}}{445})^{0.67}$
Air separation unit [O_2 production rate, m_{O2}(kg/s)] [44]	$C_{ASU} = 2.926e^{7}(\frac{m_{O2}}{28.9})^{0.7}$
Oxygen pressure booster pump [Break power output $\dot{W}_{OP,BRK}$(kW), Isentropic efficiency η_{OP}(-)] [45]	$C_{OP} = 623.22\ (\dot{W}_{OP,BRK})^{0.95}(1 + \frac{0.2}{1-\eta_{OP}})$
Turbine [Break power output, $\dot{W}_{T,BRK}$ (kW)] [46]	$C_T = 3744.3\ (\dot{W}_{T,BRK})^{0.7} - 61.3\ (\dot{W}_{T,BRK})^{0.95}$
Generator [Break power output, $\dot{W}_{T,BRK}$(kW) [46]	$C_{Gen} = 26.18\ (\dot{W}_{T,BRK})^{0.95}$

The capital costs associated with the SOF-NGCC bottoming cycle and the power cycle of the CLC-sCO2, both of which are sCO2 cycles, are determined from the capital cost correlations for each specific piece of equipment as outlined below. To estimate the costs of the sCO2 turbine and compressor, the methodology presented by Benjelloun et al. [47] is used. Eqs. (5) and (6), respectively, relate the capital cost of the turbine and compressor to their operating parameters, such as mass flow rate ($\dot{m}$), pressure ratio (β), isentropic efficiency η (η) η and turbine inlet temperature ($T_{T,i}$). Eq. (7), which is taken from Gabbrielli and Singh [48], is used to calculate the capital cost of any type of heat exchanger. This capital cost depends on the surface area (A_{HE}) and the operating pressure (P_{HE}) of the particular heat exchanger.

$$C_T = \dot{m}_T \cdot \beta\ .\left(\frac{392.2}{1-\eta_T}\right) \cdot ln(\beta)\left(1 + \exp\left(0.036\ T_{T,i} - 65.66\right)\right) \quad (5)$$

$$C_C = \dot{m}_C \left(\frac{47.1}{0.92 - \eta_C}\right) \beta_C .\ ln(\beta_C) \quad (6)$$

$$C_{HE} = 2546.9 \cdot {A_{HE}}^{0.67} \cdot {P_{HE}}^{0.28} \quad (7)$$

The capital cost of the CO_2 pump is estimated using Eq. (8) [48] that considers the brake power ($\dot{W}_p$) and isentropic efficiency ($\eta_{i,P}$).

$$C_P = 3531.4 \cdot \dot{W}_P{}^{0.71} \cdot \left[1 + \left(\frac{1-0.8}{1-\eta_{i,P}}\right)^3\right] \quad (8)$$

4. Results and Discussion

4.1. Thermodynamic performance

The thermodynamic assessment of the CLC-sCO_2, considering initial design parameters presented in Table 1, revealed that this cycle has a net power output of 380.3 MW. Such output corresponded to a net efficiency of 49.3%. The detailed performance summary of the CLC-sCO_2 is shown in Table 5. As can be observed, a considerable share of total system energy input (26.4%) is utilised for the sCO_2 compression stage (compressor and pump).

Table 5. Performance summary of CLC-sCO_2

Component	Value
Thermal energy input (MW)	768.3
s-CO_2 turbine power output (MW)	609.6
Air compression power consumption (MW)	5.4
s-CO_2 cycle compression stage power consumption (MW)	203
CO_2 compression for storage power consumption (MW)	23.6
Net power output (MW)	377.6
Net efficiency (%)	49.1

The thermodynamic performance of the proposed process is directly dependent on the performance of the closed sCO_2 cycle. Therefore, a parametric study of the CLC-sCO_2 was performed by varying the sCO_2 turbine inlet temperature (TIT) and turbine inlet pressure (TIP). In addition, in the sCO_2 cycle, there is an imbalance in the specific heat of the hot- and cold-side of the recuperator [49], as the specific heat of the sCO_2 stream is higher at the condition of low temperature and high pressure [50]. This difference results in a pinch point problem [26].To compensate for this imbalance, the sCO_2 stream is split after the LTR, as shown in Figure 2b. Recompressing one stream without heat rejection [51] compensates for this imbalance, reducing the amount of waste heat in the system, and subsequently leading to a higher net efficiency. Thus, the effect of the split fraction (SF) on the net efficiency is analysed.

Figure 3 shows the variation in the CLC-sCO_2 net efficiency with split fraction. The split fraction varies from 0.25 to 0.4, indicating the fraction of total flow entering the HTR. Figure 3 reveals that the maximum efficiency is achieved when the split fraction is 0.38. This is because, at this split fraction, the approach temperature is minimised at both ends of the LTR, maximising the heat transfer rate.

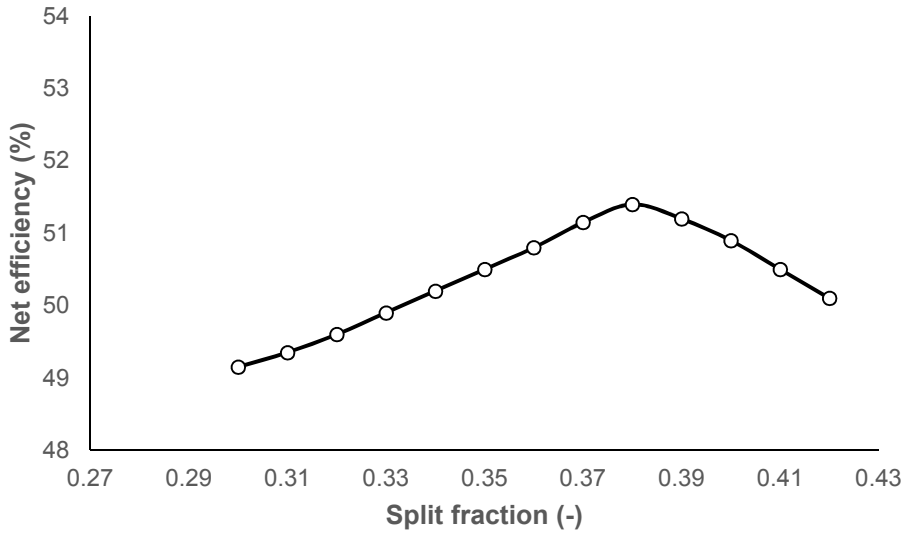

Figure 3. Effect of split fraction on the net efficiency

The effect of the sCO_2 TIT and TIP on the net efficiency of the cycle is presented in Figure 4. This parametric analysis indicated that the net efficiency of the cycle is correlated to the sCO_2 TIT and TIP. It can be seen that the correlation with the temperature is nearly linear (Figure 4a) while that with the pressure is of the second order (Figure 4b). The highest TIT of the sCO_2 cycle in this study is set at 700°C, considering the cost and lifetime of the materials under high-pressure and high-temperature conditions. Operation under such conditions was found to result in a net efficiency of 51.4%. However, further development of materials for high-temperature application would enable even higher efficiencies as further increase in TIT to 800°C resulted in a net efficiency of 55.5%. On the other hand, the analysis of the net efficiency trend in Figure 4b indicates that an increase in TIP from 200 bar to 240 bar has a more pronounced effect on the cycle performance (efficiency increases from 49.1% to 50.6%) than that from 240 bar to 300 bar (efficiency increases from 50.6% to 51.4%). It needs to be highlighted, however, that such trends for temperature and pressure, respectively, are in agreement with the results reported for sCO_2 cycles in different applications [52].

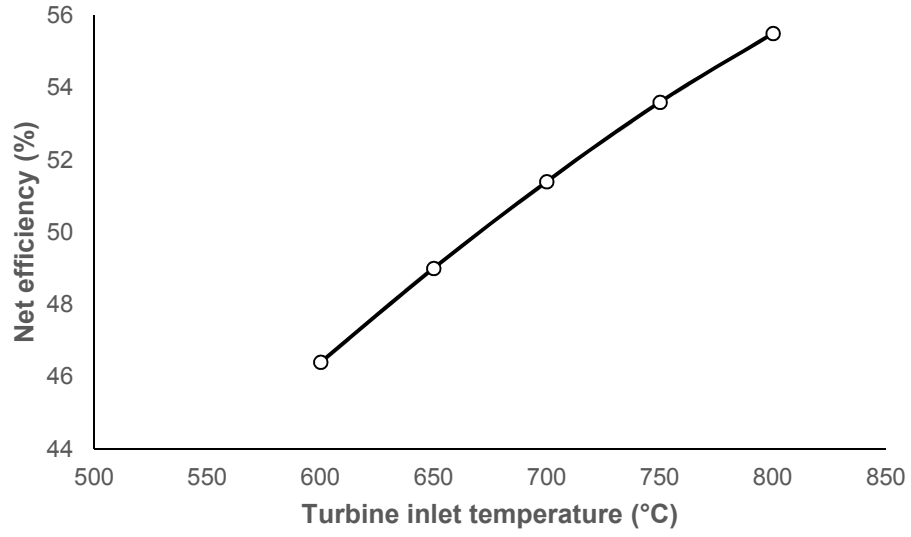

a)

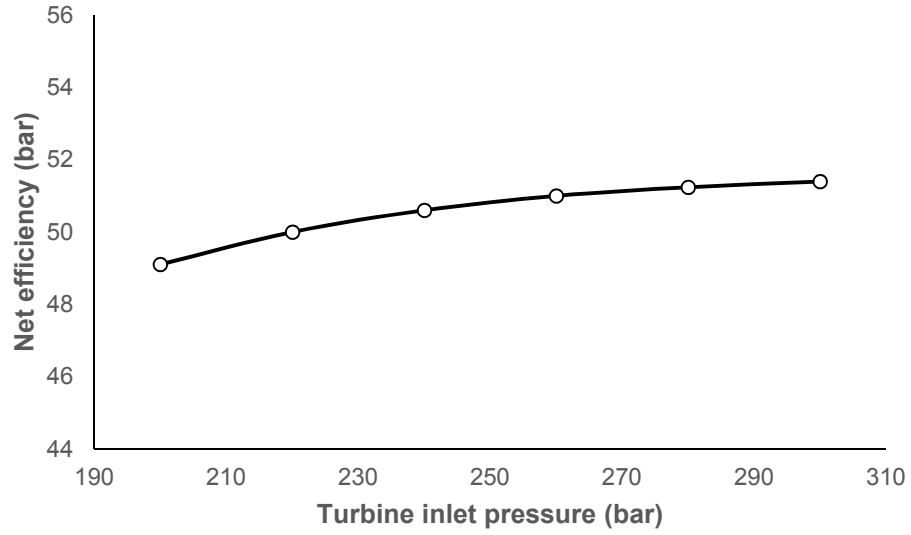

b)

Figure 4. Effect of sCO_2 turbine inlet a) temperature, and b) pressure, on the net efficiency

4.2. Techno-economic performance comparison

The thermodynamic performance of the SOF-NGCC and the CLC-sCO_2 is summarised in Table 6. The same natural gas input (59470 kg/h) is used for both cycles. The analysis shows that the CLC-sCO_2 has a net power of 395 MW (Eq. 9) with a net efficiency of 51.4%. This performance is worse than that of the state-of-the-art NGCC without CO_2 capture with a net efficiency of above 62% [53]. However, it is comparable with NGCCs with CO_2 capture as PCC implementation was reported to result in an efficiency penalty of more than 8% [54]. Importantly, the net efficiencies of other configurations of CLC have been reported as below:

- CLC integrated with the humid air turbine considered by Brandvoll and Bolland (54%) [13] and by Olaleye and Wang (57.1%) [18];
- CLC-based NGCCs comprising the conventional air turbine cycle and steam cycle considered by Mantripragada and Rubin (48.9–53.2%) [10] and Naqvi and Bolland (53%) [14]; and
- CLC-sCO_2 for combined heat and power (net power efficiency of 41.3% and total efficiency of 81.7%) proposed by Chen et al. [15].

Although the sCO_2 cycle compared to the conventional power cycles, such as the air turbine cycle and steam cycle, and advanced power cycles, such as the humid air turbine cycle, has a higher thermal efficiency, the CLC-sCO_2 in this study has lower efficiency compared to the studies above. This is mainly because of different turbomachinery assumptions considered in this study. It also needs to be highlighted that, based on the turbomachinery efficiencies considered in this study, the SOF-NGCC has a net power output of 374.1 MW (Eq. 10) with an efficiency of 48.7%, which is lower by 20.9 MW compared to that of the CLC-sCO_2. This is mainly because of the power consumption of the cryogenic ASU and subsequent O_2 compression to 300 bar, which is the combustion pressure in the SOF-NGCC. In addition, compared to the required power for CO_2 compression for storage in the CLC-sCO_2, the power consumption for CO_2 purification and compression in the SOF-NGCC is much lower, 23.6 MW and 4.0 MW, respectively. This is mainly due to the higher pressure ratio for CO_2 compression (for storage) in the CLC-sCO_2 than in the SOF-NGCC, 120 and 3.4, respectively. It is worth mentioning that there is a slight difference in the CO_2 purity for storage in both cycles, 96.7% for CLC-sCO_2 and 97.6% for SOF-NGCC. This is mainly because of CPU implementation in the SOF-NGCC case. Importantly, the thermodynamic assessment of the CLC-sCO_2 considered in this study indicates that such concept could be a feasible option that would support achieving the emission reduction targets by 2050. Importantly, when natural gas is substituted with biogas, such concept will become carbon negative. Yet, the economic feasibility of such concept needs to be proven.

Table 6. Thermodynamic performance comparison between CLC-sCO$_2$ and SOF-NGCC

Component	CLC-sCO$_2$	SOF-NGCC
Thermal energy input (MW)	768.3	768.3
High-pressure turbine power output, W_1 (MW)	-	64.4
sCO$_2$ turbine power output, W_2 (MW)	658.7	576.7
Natural gas compressor power consumption, W_3 (MW)	-	3.8
Air separation unit power consumption, W_4 (MW)	-	51.9
Air/O$_2$ compression power consumption, W_5 (MW)	5.4	41.4
sCO$_2$ compression stage power consumption, W_6 (MW)	234.7	165.9
CO$_2$ purification and compression power consumption, W_7 (MW)	-	4.0
CO$_2$ compression (for storage) power consumption, W_8 (MW)	23.6	-
Gross power output, W_{gross} (MW)	424.0	475.2
Net power output, W_{net} (MW)	395.0	374.1
Net efficiency (%)	51.4	48.7

$$\boldsymbol{W_{net,\ CLC-sCO_2} = W_2 - W_5 - W_6 - W_8} \quad (9)$$

$$\boldsymbol{W_{net,\ SOF-NGCC} = W_1 + W_2 - W_3 - W_4 - W_5 - W_6} \quad (10)$$

$$\boldsymbol{W_{gross,\ CLC-sCO_2} = W_2 - W_6} \quad (11)$$

$$\boldsymbol{W_{gross,\ SOF-NGCC} = W_1 + W_2 - W_6} \quad (12)$$

The results presented in Table 5 are used as the inputs in the economic assessment of both the SOF-NGCC and CLC-sCO$_2$. Using these inputs, the LCOE has been calculated to assess the economic feasibility of the considered cases. The breakdown of the capital cost for both considered cases is shown in Figure 5a and Figure 5b. The capital cost of the CLC-sCO$_2$ is lower by £2M than that of the SOF-NGCC (£323M and £325M, respectively). The capital cost associated with the CLC reactors is almost 4 times as high as that associated with the combustors implemented in the SOF-NGCC (£41.3M and £10.8M, respectively). In addition, the higher pressure ratio of the CO$_2$ compressor for storage in the CLC-sCO$_2$ compared to the SOF-NGCC results in that compressor being more than 4 times as expensive as the corresponding unit in the SOF-NGCC (£42.2M and £9.4M, respectively). However, the cost associated with the ASU in the SOF-NGCC (£53M) results in higher capital cost of SOF-NGCC compared to CLC-sCO$_2$. It is worth pointing out that in both cycles, the cost associated with turbines and pumps has the highest contribution to the total capital cost.

Importantly, the specific capital cost of the CLC-sCO_2 and the SOF-NGCC are estimated to be £761/kW_{gross} and £684/kW_{gross}. Such specific capital costs are comparable with the range reported for NGCCs without CO_2 capture (£400/kW_{gross}–£700/kW_{gross}) and figures reported for NGCCs with CO_2 capture (£730/kW_{gross}–£1010/kW_{gross}) [34] . This indicates that both cycles are economically competitive to more mature technologies.

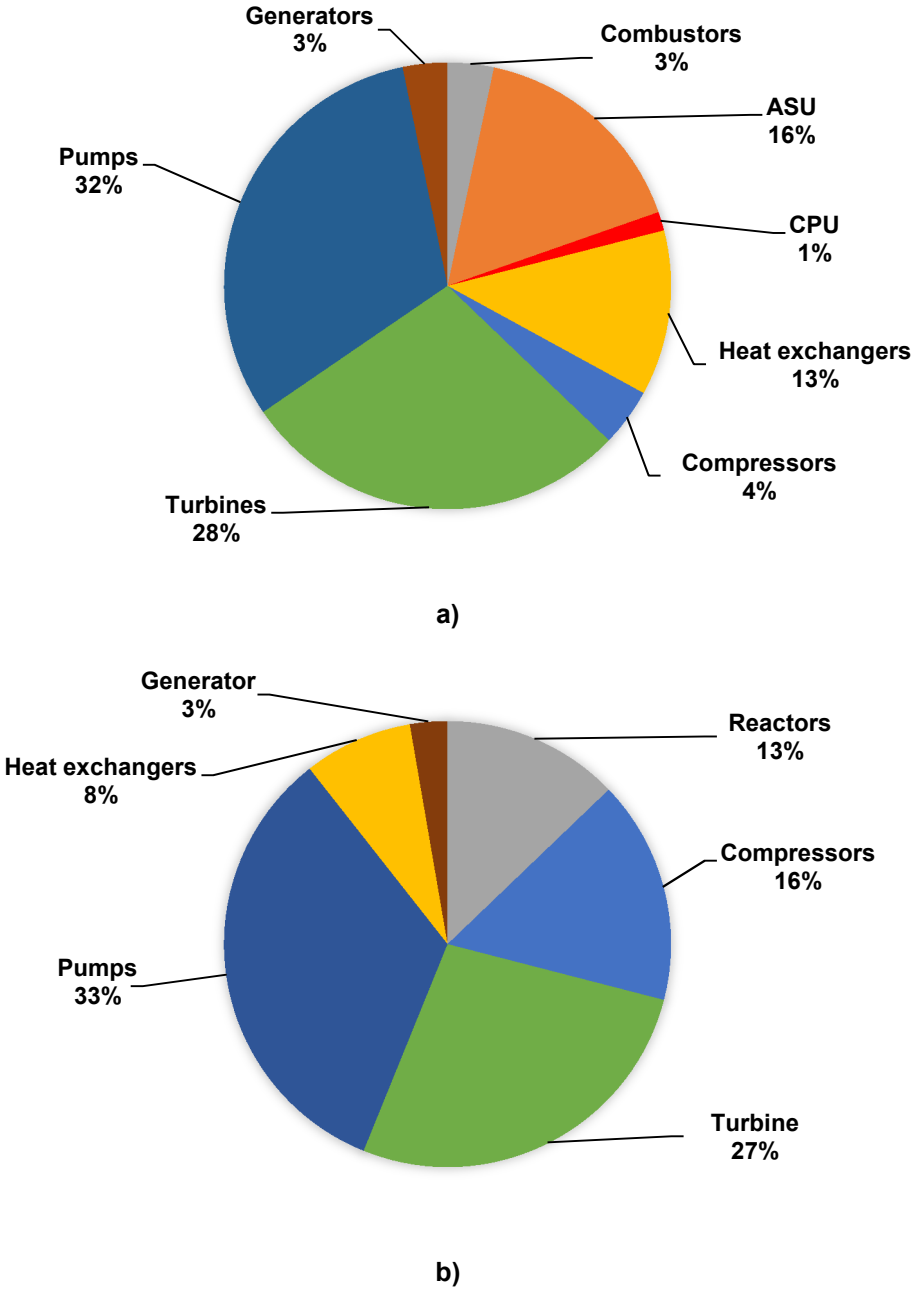

Figure 5. Breakdown of the capital cost for a) SOF-NGCC and b) CLC-sCO_2

The LCOE for the CLC-sCO_2 is £36.1/MWh, compared to £38.3/MWh for the reference SOF-NGCC cycle. This is because of the lower capital cost and higher net efficiency

of the CLC-sCO_2 compared to those of the SOF-NGCC, which results in lower fuel costs per unit of generated power. The LCOE of the CLC-sCO_2 (£36.1/MWh) is within the range reported for conventional fossil fuel power plants (£28/MWh–£55/MWh) [34] . It also needs to be highlighted that it is almost half of the cost of electricity considered for CLC with the humid air turbine (£77.5/MWh). In addition, it is superior to the LCOE of the Allam cycle (£50/MWh) [55] which is known to have the best performance among all NG-fired oxy-combustion cycles with the maximum net efficiency of 55.1% [56] and 54.6% [57] and other fossil fuel power plants with CO_2 capture (£39/MWh–£78/MWh) [34]. Therefore, further development of the CLC-sCO_2 would contribute to decarbonisation of the power sector at an affordable cost.

5. Conclusions

This study presents a novel concept of gas firing using chemical looping combustion (CLC) for oxygen supply rather than an air separation unit (ASU) in oxy-combustion systems, and the supercritical CO_2 cycle for power generation (CLC-sCO_2). A process model of the proposed system was developed in Aspen Plus®, and a parametric study was conducted by varying the inlet sCO_2 turbine conditions and split fraction to achieve the optimal performance of the CLC-sCO_2. This was followed by an economic assessment to evaluate the economic performance of the CLC-sCO_2 and staged oxy-fuel natural gas combined cycle (SOF-NGCC). It was found that the CLC-sCO_2 is characterised with a net efficiency of 51.4%, which is higher than the SOF-NGCC, which was considered as a reference, with a net efficiency of 48.7%. Lower capital cost of the CLC-sCO_2 compared to that of the SOF-NGCC (£323M and £325M, respectively), along with its lower power consumption, mainly due to no ASU, results in lower levelised cost of electricity (LCOE) by £2.2/MWh (£36.1/MWh and £38.3/MWh, respectively). Importantly, the techno-economic performance of the CLC-sCO_2 has been shown to be superior to other high-efficiency low-emission power generation cycles, such as the Allam cycle and CLC integrated with a humid air turbine, which attracts profound interest in its commercialisation.

List of Abbreviations

ASU	Air Separation Unit
PCC	Post-Combustion Capture
NGCC	Natural Gas Combined Cycle
SOF-NGCC	Staged Oxy-fuel Natural Gas Combined Cycle
sCO_2	Supercritical CO_2
CPU	Carbon Purification Unit
CLC	Chemical Looping Combustion
OC	Oxygen Carrier
TIT	Turbine Inlet Temperature
TIP	Turbine Inlet Pressure
LCOE	Levelised Cost of Electricity
CCS	Carbon Capture and Storage
SOFC	Solid Oxide Fuel Cell
EGR	Exhaust Gas Recycle

Nomenclature

A_{HE}	Heat exchanger surface area [m^2]
C_j	Capital cost of equipment j [£]
CF	Capacity factor [-]
FCF	Fixed charge factor [-]
FOM	Fixed operating and maintenance cost [£]
LCOE	Levelised cost of electricity [£/MWh]
LHV	Lower heating value [kJ/kg]
$\dot{m}_{fuel}$	Fuel consumption rate [kg/s]
$\dot{m}_{O_2}$	O_2 production rate in air separation unit [kg/s]
P_{HE}	Heat exchanger operating pressure [bar]
r	Project interest rate (%)
SFC	Specific fuel cost [£/MWh]
T	Project lifetime (years)
TCR	Total capital requirement [£]

T_{T_i}	Turbine inlet temperature [°C]
VOM	Variable operating and maintenance cost [£/MWh]
$\dot{W}_{j,BRK}$	Break power output/requirement of equipment j [kW]
$\dot{W}_{net}$	Net power output [kW]
η_j	Isentropic efficiency of equipment j [%]
η_{net}	Thermal efficiency [%]
β	Pressure ratio [-]

References

[1] Kanniche M, Gros-Bonnivard R, Jaud P, Valle-Marcos J, Amann J.M, Bouallou C. Pre-combustion, post-combustion and oxy-combustion in thermal power plant for CO_2 capture. Appl Therm Eng 2010;30:53–62. doi:10.1016/j.applthermaleng.2009.05.005.

[2] Wu F, Argyle M.D, Dellenback P.A, Fan M. Progress in O_2 separation for oxy-fuel combustion– A promising way for cost-effective CO_2 capture: A review. Prog Energy Combust Sci 2018;67:188–205. doi:10.1016/j.pecs.2018.01.004.

[3] Higginbotham P, White V, Fogash K, Guvelioglu G. Oxygen supply for oxyfuel CO_2 capture. Int J Greenh Gas Control 2011;5:S194–203. doi:10.1016/j.ijggc.2011.03.007.

[4] Wankat P.C, Kostroski K.P. Hybrid air separation processes for production of oxygen and nitrogen. Sep Sci Technol 2010;45:1171–85. doi:10.1080/01496391003745728.

[5] Chorowski M, Gizicki W. Technical and economic aspects of oxygen separation for oxy-fuel purposes. Arch Thermodyn 2015;36:157–70. doi:10.1515/aoter-2015-0011.

[6] Zhou C, Shah K, Moghtaderi B. Techno-economic assessment of integrated chemical looping air separation for oxy-fuel combustion : An Australian case study. Energy & Fuels 2015;29:2074−2088. doi:10.1021/ef5022076.

[7] Mattisson T, Lyngfelt A, Cho P. The use of iron oxide as an oxygen carrier in chemical-looping combustion of methane with inherent separation of CO_2. Fuel 2001;80:1953–62. doi:10.1016/S0016-2361(01)00051-5.

[8] Porrazzo R, White G, Ocone R. Fuel reactor modelling for chemical looping combustion: From micro-scale to macro-scale. Fuel 2016;175:87–98. doi:10.1016/j.fuel.2016.01.041.

[9] Abanades J.C, Arias B, Lyngfelt A, Mattisson T, Wiley D.E, Li H, Ho M.T, Mangano E, Brandani S. Emerging CO_2 capture systems. Int J Greenh Gas Control 2015;40:126–66. doi:10.1016/j.ijggc.2015.04.018.

[10] Mantripragada H.C, Rubin E.S. Performance model for evaluating chemical looping combustion (CLC) processes for CO_2 capture at gas-fired power plants. Energy & Fuels 2016;30:2257–67. doi:10.1021/acs.energyfuels.5b02441.

[11] Källén M, Rydén M, Dueso C, Mattisson T, Lyngfelt A. $CaMn_{0.9}Mg_{0.1}O_{3-\delta}$ as oxygen carrier in a gas-fired 10 kW th chemical-looping combustion unit. Ind Eng Chem Res 2013;52:6923–32. doi:10.1021/ie303070h.

[12] Källén M, Rydén M, Lyngfelt A, Mattisson T. Chemical-looping combustion using combined iron/manganese/silicon oxygen carriers. Appl Energy 2015;157:330–7. doi:10.1016/j.apenergy.2015.03.136.

[13] Brandvoll O, Bolland O. Inherent CO_2 capture using chemical looping combustion in a natural gas fired power cycle. J Eng Gas Turbines Power 2004;126:316. doi:10.1115/1.1615251.

[14] Naqvi R, Bolland O. Multi-stage chemical looping combustion (CLC) for combined cycles with CO_2 capture. Int J Greenh Gas Control 2007;1:19–30. doi:10.1016/S1750-5836(07)00012-6.

[15] Chen S, Soomro A, Yu R, Hu J, Sun Z, Xiang W. Integration of chemical looping combustion and supercritical CO_2 cycle for combined heat and power

generation with CO_2 capture. Energy Convers Manag 2018;167:113–24. doi:10.1016/j.enconman.2018.04.083.

[16] Spallina V, Nocerino P, Romano M.C, van Sint Annaland M, Campanari S, Gallucci F. Integration of solid oxide fuel cell (SOFC) and chemical looping combustion (CLC) for ultra-high efficiency power generation and CO_2 production. Int J Greenh Gas Control 2018;71:9–19. doi:10.1016/j.ijggc.2018.02.005.

[17] Hamers H.P, Romano M.C, Spallina V, Chiesa P, Gallucci F, van Sint Annaland M. Energy analysis of two stage packed-bed chemical looping combustion configurations for integrated gasification combined cycles. Energy 2015;85:489–502. doi:10.1016/j.energy.2015.03.063.

[18] Olaleye A.K, Wang M. Techno-economic analysis of chemical looping combustion with humid air turbine power cycle. Fuel 2014;124:221–31. doi:10.1016/j.fuel.2014.02.002.

[19] Hanak DP, Manovic V. Calcium looping with supercritical CO_2 cycle for decarbonisation of coal-fired power plant. Energy 2016;102:343–53. doi:10.1016/j.energy.2016.02.079.

[20] Gopan A, Kumfer B.M, Phillips J, Thimsen D, Smith R, Axelbaum R.L. Process design and performance analysis of a staged, pressurized oxy-combustion (SPOC) power plant for carbon capture. Appl Energy 2014;125:179–88. doi:10.1016/j.apenergy.2014.03.032.

[21] Gopan A, Kumfer B.M, Axelbaum R.L. Effect of operating pressure and fuel moisture on net plant efficiency of a staged, pressurized oxy-combustion power plant. Int J Greenh Gas Control 2015;39:390–6. doi:10.1016/j.ijggc.2015.05.014.

[22] Xia F, Yang Z, Adeosun A, Gopan A, Kumfer B.M, Axelbaum R.L. Pressurized oxy-combustion with low flue gas recycle: Computational fluid dynamic simulations of radiant boilers. Fuel 2016;181:1170–8. doi:10.1016/j.fuel.2016.04.023.

[23] Khallaghi N, Hanak D.P, Manovic V. Staged oxy-fuel natural gas combined

cycle. Appl Therm Eng 2019;153:761–7. doi:10.1016/j.applthermaleng.2019.03.033.

[24] Adnan M.A, Azis M.M, Quddus M.R, Hossain M.M. Integrated liquid fuel based chemical looping combustion–parametric study for efficient power generation and CO_2 capture. Appl Energy 2018;228:2398–406. doi:10.1016/j.apenergy.2018.07.072.

[25] Khan M.N, Shamim T. Investigation of hydrogen generation in a three reactor chemical looping reforming process. Appl Energy 2016;162:1186–94. doi:10.1016/j.apenergy.2015.08.033.

[26] Padilla R.V, Soo Too Y.C, Benito R, Stein W. Exergetic analysis of supercritical CO_2 Brayton cycles integrated with solar central receivers. Appl Energy 2015;148:348–65. doi:10.1016/j.apenergy.2015.03.090.

[27] Turchi C.S, Ma Z, Neises T, Wagner M. Thermodynamic study of advanced supercritical carbon dioxide power cycles for high performance concentrating solar power systems. ASME 2012 6th Int Conf Energy Sustain Parts A B 2012;135:375. doi:10.1115/ES2012-91179.

[28] Le Moullec Y. Conceptual study of a high efficiency coal-fired power plant with CO_2 cature using a supercritical CO_2 Brayton cycle. Energy 2013;49:32–46. doi:10.1016/j.energy.2012.10.022.

[29] Adánez-Rubio I, Arjmand M, Leion H, Gayán P, Abad A, Mattisson T, Lyngfelt A. Investigation of combined supports for cu-based oxygen carriers for chemical-looping with oxygen uncoupling (CLOU). Energy and Fuels 2013;27:3918–27. doi:10.1021/ef401161s.

[30] Adanez J, Abad A, Garcia-Labiano F, Gayan P, De Diego L.F. Progress in chemical-looping combustion and reforming technologies. Prog Energy Combust Sci 2012;38:215–82. doi:10.1016/j.pecs.2011.09.001.

[31] Manovic V, Anthony E.J. Integration of calcium and chemical looping combustion using composite CaO/CuO-based materials. Environ Sci Technol 2011;45:10750–6. doi:10.1021/es202292c.

[32] Zheng J.Y, Van T-K, Pawar A.U, Kim C.W, Kang Y.S. One-step transformation

of Cu to Cu_2O in alkaline solution. RSC Adv 2014;4:18616. doi:10.1039/c4ra01174k.

[33] Santini L, Accornero C, Cioncolini A. On the adoption of carbon dioxide thermodynamic cycles for nuclear power conversion: A case study applied to Mochovce 3 Nuclear Power Plant. Appl Energy 2016;181:446–63. doi:10.1016/j.apenergy.2016.08.046.

[34] Hanak D.P, Jenkins B.G, Kruger T, Manovic V. High-efficiency negative-carbon emission power generation from integrated solid-oxide fuel cell and calciner. Appl Energy 2017;205:1189–201. doi:10.1016/j.apenergy.2017.08.090.

[35] Michalski S, Hanak D.P, Manovic V. Techno-economic feasibility assessment of calcium looping combustion using commercial technology appraisal tools. J Clean Prod 2019;219:540–51. doi:10.1016/j.jclepro.2019.02.049.

[36] Moisseytsev A, Sienicki J.J. Investigation of alternative layouts for the supercritical carbon dioxide Brayton cycle for a sodium-cooled fast reactor. Nucl Eng Des 2009;239:1362–71. doi:10.1016/j.nucengdes.2009.03.017.

[37] Mantripragada H.C, Rubin E.S. Chemical looping for pre-combustion CO_2 capture — performance and cost analysis. Energy Procedia 2013;37:618–25. doi:10.1016/j.egypro.2013.05.149.

[38] Lyngfelt A, Leckner B, Mattisson T. A fuidized-bed combustion process with inherent CO_2 separation; application of chemical-looping combustion. Chem Eng Sci 2001;56:3101–13.

[39] Peters M.S, Timmerhaus K.D. Plant design and economics for engineers. 4th ed. McGraw-Hill; 1991.

[40] NRE. Equipment design and cost estimation for small modular biomass systems, synthesis gas cleanup, and oxygen separation equipment. San Francisco. 2006.

[41] López R, Fernández C, Martínez O, Sánchez M.E. Techno-economic analysis of a 15 MW corn-rape oxy-combustion power plant. Fuel Process Technol 2016;142:296–304. doi:10.1016/j.fuproc.2015.10.020.

[42] Shirazi A, Aminyavari M, Najafi B, Rinaldi F, Razaghi M. Thermal-economic-environmental analysis and multi-objective optimization of an internal-reforming solid oxide fuel cell-gas turbine hybrid system, Int. J. of Hydrogen Energy , 37 (24), 2012, pp 19111–19124. doi:10.1016/j.ijhydene.2012.09.143.

[43] Lee Y.D, Ahn K.Y, Morosuk T, Tsatsaronis G. Exergetic and exergoeconomic evaluation of a solid-oxide fuel-cell-based combined heat and power generation system. Energy Convers Manag 2014;85:154–64. doi:10.1016/j.enconman.2014.05.066.

[44] Atsonios K, Koumanakos A, Panopoulos K.D, Doukelis A, Kakaras E. Techno-economic comparison of CO_2 capture technologies employed with natural gas derived GTCC. Proc. ASME Turbo Expo, San Antonio, Texas, USA: 2013.

[45] Khoshgoftar Manesh M.H, Ghalami H, Amidpour M, Hamedi M.H. Optimal coupling of site utility steam network with MED-RO desalination through total site analysis and exergoeconomic optimization. DES 2013;316:42–52. doi:10.1016/j.desal.2013.01.022.

[46] Aminyavari M, Haghighat Maghami A, Shirazi A, Najafi B, Rinaldi F. Exergetic, economic, and environmental evaluations and multi-objective optimization of an internal-reforming SOFC-gas turbine cycle coupled with a Rankine cycle. Appl Therm Eng 2016;108:833–46. doi:10.1016/j.applthermaleng.2016.07.180.

[47] Benjelloun M, Doulgeris G, Singh R. A method for techno-economic analysis of supercritical carbon dioxide cycles for new generation nuclear power plants. Proc Inst Mech Eng Part A J Power Energy 2012;226:372–83. doi:10.1177/0957650911429643.

[48] Gabbrielli R, Singh R. Economic and scenario analyses of new gas turbine combined cycles with no emissions of carbon dioxide. J Eng Gas Turbines Power 2005;127:531. doi:10.1115/1.1850492.

[49] Ahn Y, Bae S.J, Kim M, Cho S.K, Baik S, Lee J.I, Cha J.e. Review of supercritical CO_2 power cycle technology and current status of research and development. Nucl Eng Technol 2015;47:647–61. doi:10.1016/j.net.2015.06.009.

[50] Wang X, Liu Q, Bai Z, Lei J, Jin H. Thermodynamic investigations of the supercritical CO_2 system with solar energy and biomass. Appl Energy 2018;227:108–18. doi:10.1016/j.apenergy.2017.08.001.

[51] Pham H.S, Alpy N, Ferrasse J.H, Boutin O, Quenaut J, Tothill M, Haubensack D, Saez M. Mapping of the thermodynamic performance of the supercritical CO_2 cycle and optimisation for a small modular reactor and a sodium-cooled fast reactor. Energy 2015;87:412–24. doi:10.1016/j.energy.2015.05.022.

[52] Li H, Su W, Cao L, Chang F, Xia W, Dai Y. Preliminary conceptual design and thermodynamic comparative study on vapor absorption refrigeration cycles integrated with a supercritical CO_2 power cycle. Energy Convers Manag 2018;161:162–71. doi:10.1016/j.enconman.2018.01.065.

[53] Smith R.W. Steam turbine cycles and cycle design optimization: combined cycle power plants. Adv. Steam Turbines Mod. Power Plants, 2017, p. 57–92.

[54] Fernandez E.S, Goetheer E.L.V, Manzolini G, Macchi E, Rezvani S, Vlugt T.J.H. Thermodynamic assessment of amine based CO_2 capture technologies in power plants based on European Benchmarking Task Force methodology. Fuel 2014;129:318–29. doi:10.1016/j.apenergy.2014.04.066.

[55] Lu X. Allam cycle coal- A new clean coal power cycle. Durham, NC, USA: 2017.

[56] Ferrari N, Mancuso L, Davison J, Chiesa P, Martelli E, Romano M.C. Oxy-turbine for power plant with CO_2 capture. Energy Procedia 2017;114:471–80. doi:10.1016/j.egypro.2017.03.1189.

[57] Scaccabarozzi R, Gatti M, Martelli E. Thermodynamic analysis and numerical optimization of the NET Power oxy-combustion cycle. Appl Energy 2016;178:505–26. doi:10.1016/j.apenergy.2016.06.060.